Supplemental Figures and Legends

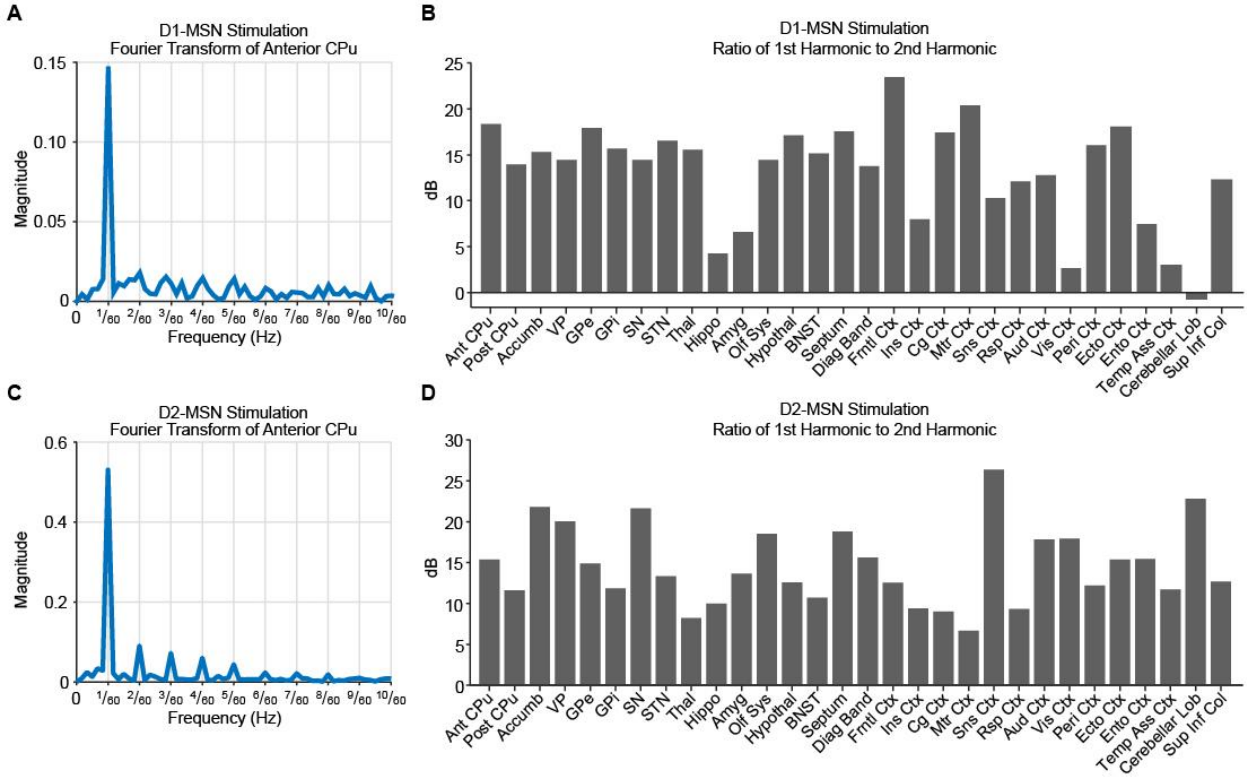

Figure S1, Related to Figure 1. Harmonic analysis of brain-wide fMRI signals confirm that modulations are primarily restricted to the fundamental frequency of repeated stimulation blocks (i.e. 1/60 Hz). A,C, Fourier transform of average fMRI time series from all voxels and animals within the left anterior CPu during D1- and D2-MSN stimulation. **B,D,** Ratio of the Fourier transform's magnitude at the fundamental frequency to its magnitude at the 2nd harmonic (i.e. 2/60 Hz) for each ROI of the left hemisphere during D1- and D2-MSN stimulation. Note that there is generally at least a 5 dB difference for all brain regions in panels B and D, suggesting that coherence analysis – by quantifying the relative power at 1/60 Hz – results in few false negatives.

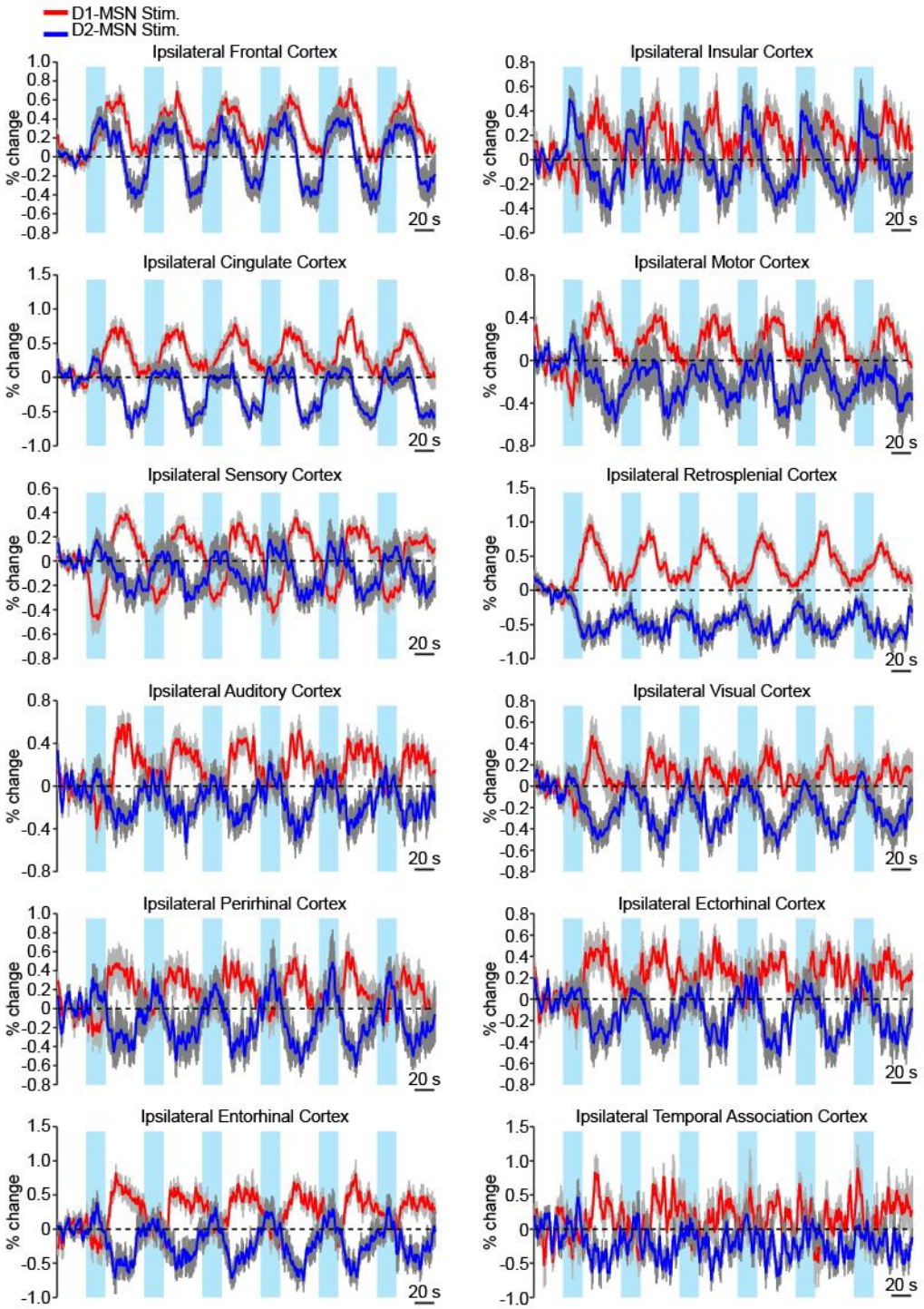

Figure S2, Related to Figure 4. fMRI time series of 12 ipsilateral cortical regions analyzed in main text show that D1- and D2-MSN stimulation evoke opposite responses throughout the ipsilateral cortex, with strong activation during D1-MSN stimulation and suppression during D2-MSN stimulation. Time series represent the average BOLD signal of active voxels within each ROI, and are expressed as the percent signal change relative to a 30 s pre-stimulation baseline period. Errorbars indicate mean ± SEM across animals. Time series were thresholded and averaged across n = 12 D1-Cre and n = 11 D2-Cre animals.

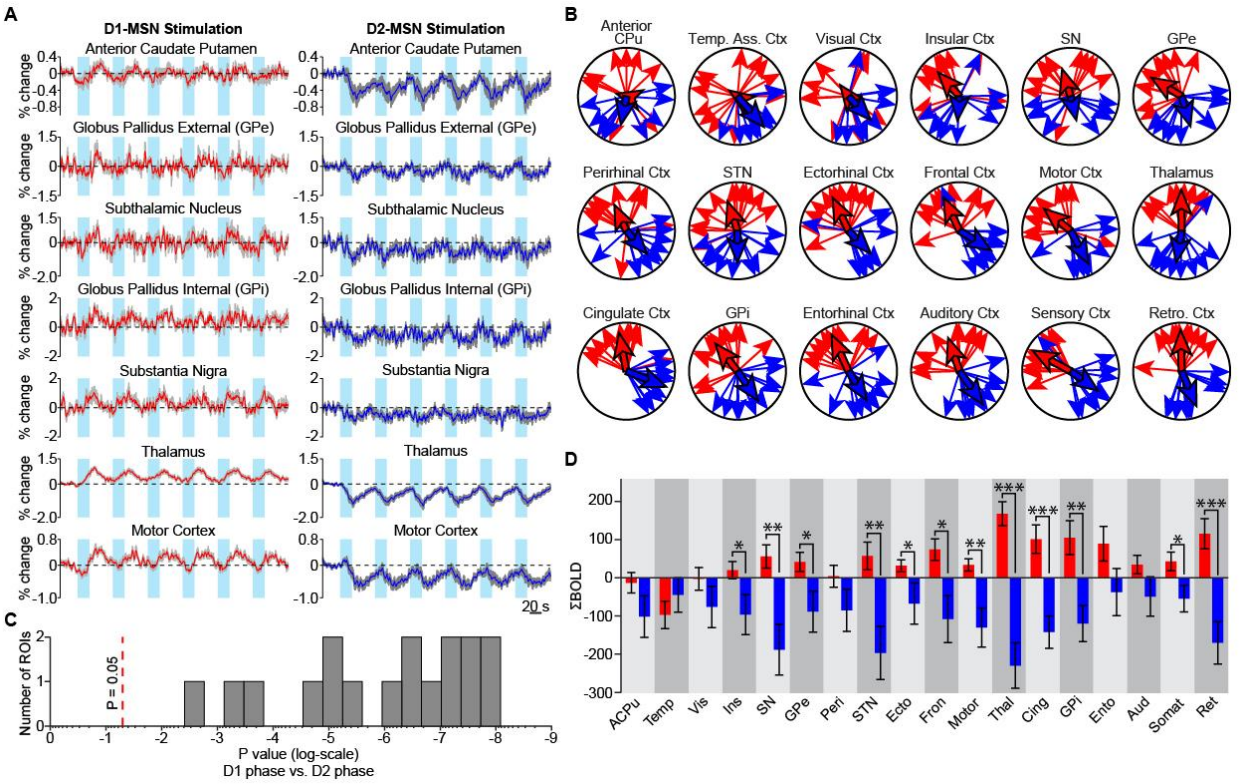

Figure S3, Related to Figure 5. Stimulations of D1- and D2-MSNs drive distinct and opposing fMRI responses in the contralateral hemisphere. A, Average BOLD signal of active voxels in the contralateral basal ganglia-thalamocortical loop thresholded from n = 12 D1-Cre and 11 D2-Cre animals. Time series values are expressed as the percent signal change relative to a 30 s pre-stimulation baseline period. Values with errorbars are mean ± SEM. **B,** Distribution of phase values within the contralateral basal ganglia-thalamocortical loop during D1- and D2-MSN stimulation. Skinny arrows indicate subject-specific values, while bolded arrows indicate the average across subjects. All regions exhibit significantly different phase values ($p < 0.001$, circular Watson-Williams test; n = 12 and 11 animals for D1- and D2-MSN stimulation, respectively) across D1- and D2-MSN stimulation responses, with the exception of the anterior caudate putamen (which did not satisfy the statistical test's assumptions). Regions are sorted by p value in descending order from left to right. **C,** Histogram of p values from circular Watson-Williams tests in panel B (excluding the anterior caudate putamen) show that phase values are significantly different between D1- and D2-MSN stimulation. **D,** Quantification of ΣBOLD values for each ROI with statistical comparisons between D1- and D2-MSN stimulation (* $p < 0.05$, ** $p < 0.005$, *** $p < 0.001$; two-tailed t-test). ΣBOLD was calculated as the summation of each ROI's average time series.

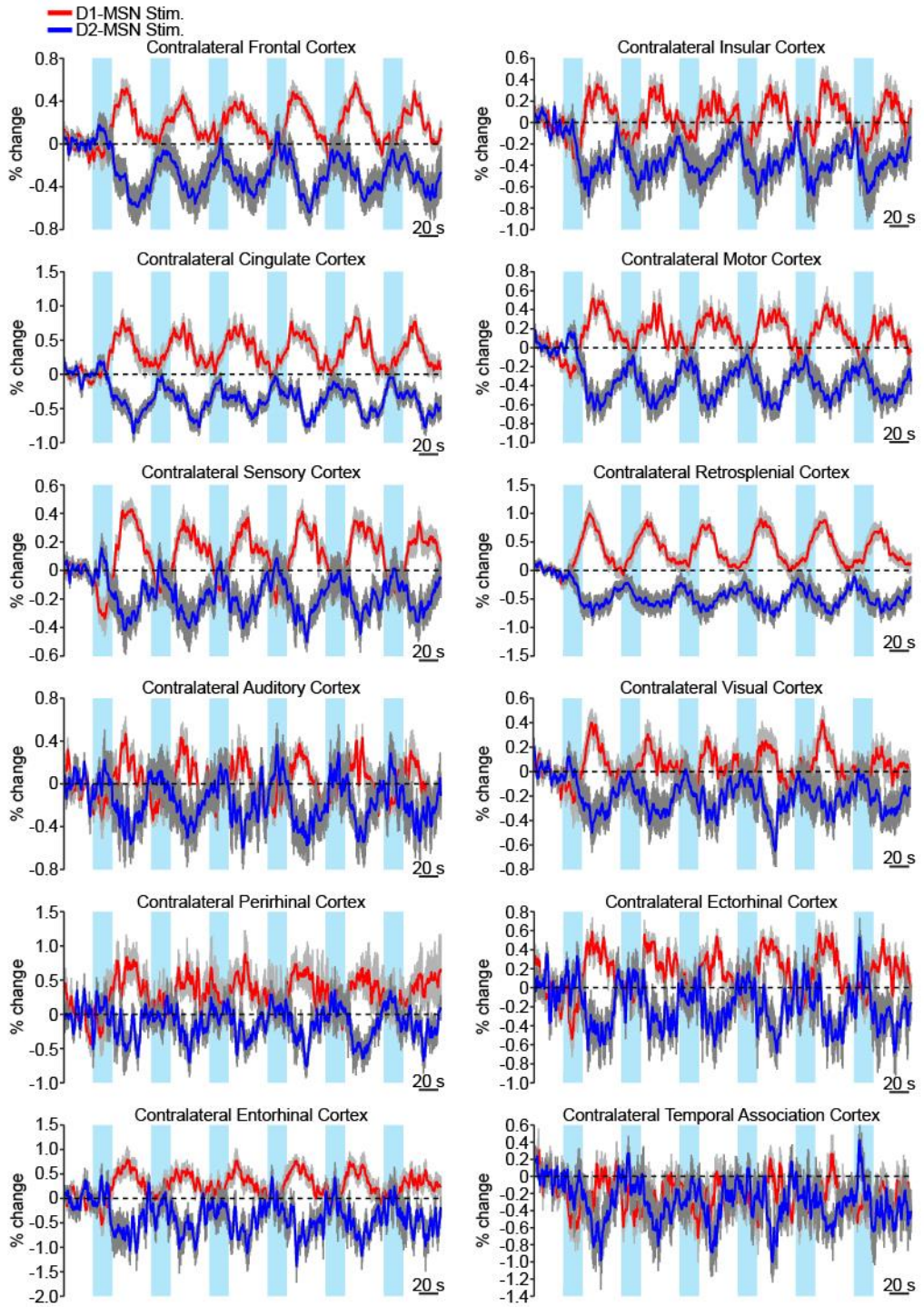

Figure S4, Related to Figure 5. fMRI time series of 12 contralateral cortical regions analyzed in Figure S3 show that D1- and D2-MSN stimulation evoke opposite responses throughout most of the contralateral cortex, with strong activation during D1-MSN stimulation and suppression during D2-MSN stimulation. Time series represent the average BOLD signal of active voxels within each ROI, and are expressed as the percent signal change relative to a 30 s pre-stimulation baseline period. Errorbars indicate mean ± SEM across animals. Time series were thresholded and averaged across n = 12 D1-Cre and n = 11 D2-Cre animals.

Supplemental Experimental Procedures

Acclimation of animals for lightly sedated fMRI

In order to facilitate fMRI under very light anesthesia conditions (0.4-0.7% isoflurane mixed with O_2 and N_2O), mice were acclimated to the fMRI procedure by gradually introducing fMRI-related phenomena and rewarding them with peanut butter delivered through a dropper. Mice underwent five cumulative stages of acclimation over the course of 14 days, ending one week before fMRI scans. Two hours of training were given each day. In the first stage of training (days 1-3), mice were rewarded for entering a forelimb/hindlimb restraining apparatus. In the second stage (days 4-5), animals were additionally restrained with scotch tape. Next (days 6-7), the head was immobilized using sponges. In the fourth stage (days 8-9), recorded noise from the fMRI pulse sequence was played back to the mice at a similar intensity (100-120 dB). For the final stage (days 10-14), no reward was given to the mice. Throughout the acclimation process, defecation and urination rates were used as indicators of stress. Respiration rates were monitored as well. 4% lidocaine was applied on the parts of the restraining apparatus that came into contact with the animal's limbs. To further minimize discomfort, gauze pads were placed between the restraining apparatus and animal's ventral surface.

ofMRI experiment and fMRI data analysis

Animals were initially anesthetized in an induction chamber with 5% isoflurane before placement into the restraining apparatus described above. The restrained animal was then placed onto a custom-made MRI-compatible cradle with ears, teeth, and head secured. A custom-designed receiver coil was placed on top of the head and centered over the region of interest to maximize signal-to-noise ratio. During fMRI scanning, animals were placed into the iso-center of the magnet while very lightly anesthetized with a calibrated vaporizer using a mixture of O_2 (35%), N_2O (65%), and isoflurane (0.4-0.7%). Body temperature was maintained at 36-38 °C using heated airflow. T2-weighted high-resolution anatomical images were acquired prior to fMRI to check for brain damage and confirm an accurate probe location. Gradient recalled echo (GRE) BOLD methods were used to acquire fMRI images during photostimulation. The fMRI image acquisition was designed to have 25×25 mm^2 in-plane field of view (FOV) and 0.36×0.36×0.5 mm^3 spatial resolution with a sliding window reconstruction to update the image every repetition time (TR) (Fang and Lee, 2013). The two-dimensional, multi-slice gradient-echo sequence used a four-interleave spiral readout (Glover and Lee, 1995; Kim et al., 2003), 750 ms TR, and 12 ms echo time, resulting in 23 coronal slices. The spiral k-space samples were reconstructed through a 2-dimensional gridding reconstruction method (Jackson et al., 1991). Finally, real-time motion correction was performed using a custom-designed GPU-based system (Fang and Lee, 2013).

All fMRI data processing was performed in Matlab (MathWorks, Inc., Natick, MA). The signal quality of each scan's motion-corrected image was first quantified by calculating the average coherence value at the site of stimulation (see below). For each scanning session, the best N motion-corrected images were averaged together, with N typically being 14 and no less than 10. The average image for each animal was then aligned to a common coordinate system using a six degree-of-freedom rigid body transformation.

Prior to time series analysis, images were spatially smoothened in 3D with a four-voxel full width at half maximum filter using SPM12. Time series were calculated for each voxel as the percent modulation of the BOLD signal relative to a 30 s baseline period collected prior to stimulation. After temporal detrending to correct for possible scanner drift and mean-subtraction, a coherence value was calculated for each voxel's time series as the magnitude of its Fourier transform at the frequency of repeated stimulation blocks (i.e. 1/60 Hz) divided by the sum-of-squares of all frequency components (Bandettini et al., 1993; Lee et al., 2010). Phase values were also calculated for each voxel as the argument of the time series' Fourier transform at the frequency of repeated stimulation blocks. This value represents the temporal shift of the response when it is modeled as a sinusoid, which accurately captured the dynamics of evoked fMRI responses in the current experiments (Figure 5A).

Active voxels were identified as those with a coherence greater than 0.35. Assuming Gaussian noise, the p value for this threshold can be estimated to be less than 10^{-9} after applying a Bonferroni correction for all brain-masked voxels (Bandettini et al., 1993). Time series displayed in Figures 4/6/7, and Figures S2/3/4 were generated by averaging the mean time series of active voxels in the corresponding region of interest (ROI) across animals. Time series in Figure 5A were averaged over all voxels within an ROI, corresponding to the calculation of phase and ΣBOLD. To generate activation maps in Figure 1, two group-wise datasets were generated by averaging together the images from all animals in the D1- or D2-MSN stimulation groups. These datasets were then processed according to the Fourier

domain analyses described above. Coherence-masked phase values were overlaid onto a corresponding T2-weighted anatomical scan and masked with a digital standard mouse brain atlas (Paxinos and Franklin, 2001).

Opsin expression validation

To confirm the precise targeting of ChR2 to D1- or D2-MSNs, a cohort of mice injected with the DIO-recombinant virus in dorsomedial striatum was deeply anesthetized with isoflurane and transcardially perfused with 0.1M PBS followed by ice-cold 4% paraformaldehyde (PFA) in PBS. Brains were extracted and fixed in 4% PFA overnight at 4 °C. The brains were equilibrated in 10%, 20%, and then 30% sucrose in PBS at 4 °C. Coronal sections of 40 (DARPP-32) or 30 (ppENK, prodynorphin) μm thickness were prepared on a freezing microtome (HM 430 Sliding Microtome, Thermo Scientific Inc.). For immunohistochemistry, free floating sections were processed with 1-2% normal donkey serum (NDS) wash buffer, and blocked and permeabilized with 5% NDS plus 0.2% Triton X-100 in PBS for 1 hr at room temperature. Sections were then exposed to primary antibodies at 4 °C for 48 hours. After washing with 1-2% NDS, sections were incubated with secondary antibodies for 2 hr (prodynorphin) or overnight (DARPP-32, ppENK) at room temperature. Slices were then washed and mounted using DAPI-Fluoromount-G (SouthernBiotech, Birmingham, AL). Antibodies included (1) anti-rabbit monocolonal antibody against DARPP-32 (1:5000, Abcam Cat# ab40801 RRID:AB_731843) with secondary antibody Alexa Fluor® 555 donkey anti-rabbit (1:500, Thermo Fisher Scientific Cat# A-31572 RRID:AB_2536182), (2) anti-rabbit monoclonal antibody against pre-pro-enkephalin (ppENK; 1:200, Neuromics Cat# RA14124 RRID:AB_2532106) with secondary antibody Alexa Fluor® 555 or 647 donkey anti-rabbit (1:500, Jackson ImmunoResearch Labs Cat# 711-605-152 RRID:AB_2492288), and (3) anti-guinea pig antibody against prodynorphin (1:200-1000, Millipore Cat# AB5519 RRID:AB_2162669) with secondary antibody Alexa Fluor® 647-AffiniPure donkey anti-guinea pig IgG (1:500-1000, Jackson ImmunoResearch Labs Cat# 706-605-148 RRID:AB_2340476). All immunohistochemistry protocols were optimized. Immuno-fluorescence was assessed with a laser confocal microscope (Leica CTR 6500).

Supplemental References

Fang, Z., and Lee, J.H. (2013). High-throughput optogenetic functional magnetic resonance imaging with parallel computations. Journal of neuroscience methods *218*, 184-195.

Glover, G.H., and Lee, A.T. (1995). Motion artifacts in fMRI: comparison of 2DFT with PR and spiral scan methods. Magn Reson Med *33*, 624-635.

Jackson, J.I., Meyer, C.H., Nishimura, D.G., and Macovski, A. (1991). Selection of a convolution function for Fourier inversion using gridding [computerised tomography application]. IEEE Trans Med Imaging *10*, 473-478.

Kim, D.H., Adalsteinsson, E., and Spielman, D.M. (2003). Simple analytic variable density spiral design. Magn Reson Med *50*, 214-219.